Nuclear Physics B191 (1981) 1–25

NUCLEAR INTERACTIONS OF SUPER HIGH ENERGY COSMIC-RAYS OBSERVED IN MOUNTAIN EMULSION CHAMBERS

*Pamir Collaboration**, Mt. Fuji Collaboration*** and Chacaltaya Collaboration****

*S.G. BAYBURINA, A.S. BORISOV, K.V. CHERDYNTSEVA, Z.M. GUSEVA, V.G. DENISOVA, A.M. DUNAEVSKII, E.A. KANEVSKAYA, V.M. MAXIMENKO, S.V. PASHKOV, V.S. PUCHKOV, S.B. SHAULOV, S.A. SLAVATINSKY, M.D. SMIRNOVA, Yu.A. SMORODIN, A.V. URYSSON, N.G. ZELEVINSKAYA and G.B. ZHDANOV

The Lebedev Physical Institute, Academy of Sciences of USSR, Moscow, USSR

L.G. AFANASJEVA, L.T. BARADZEI, E.I. GOROCHOVA, I.P. IVANENKO, N.P. ILJINA, G.B. KHRISTIANSEN, T.V. LAZAREVA, A.K. MANAGADZE, E.A. MURZINA, I.V. RAKOBOLSKAYA, T.M. ROGANOVA and N.G. RYABOVA

Institute for Nuclear Physics, Moscow State University, Moscow, USSR

G.T. ZATSEPIN and R.A. MUKHAMEDSHIN

Institute for Nuclear Research, Academy of Sciences of USSR, Moscow, USSR

S.D. CANANOV, L.A. KHISANISHVILI, N.N. ROINISHVILI, M.S. SVANIDGE, J.A. TECLIASHVILI and T.V. VARSIMASHVILI

Institute of Physics, Georgian Academy of Sciences, Tbilisi, USSR

Z.A. AZIMOV, I.B. BODOJANOV, N.E. GUBAR, Yu.A. GULOV, F. NORMURADOV and Kh. SHOBARONOV

Institute of Physics and Engineering, Tajik Academy of Sciences, Dushanbe, USSR

N.A. DOBROTIN, Yu.A. EMELJANOV, Yu.T. LUKIN, B.F. SHORIN, E.G. ZAITSEVA

Institute of High Energy Physics, Kazakh Academy of Sciences, Alma-Ata, USSR

S.A. AZIMOV, A.R. DZHURAEV, E.G. MULLADJANOV, Kh. NURITDINOV, D.A. TALIPOV, I. SHAMANSUROV and T.S. JULDASHBAEV

Institute of Physics and Engineering, Uzbek Academy of Sciences, Tashkent, USSR

Z. BUJA, E. GLADYSZ, J. MAZURKIEWICZ, S. MIKOCKI, M. SZARSKA and L. ZAWIEJSKI

Institute of Nuclear Physics, Krakow, Poland

H. BIELAWSKA, R. JUSKIEWICZ, J.L. KACPERSKI, A. KRYS, J. MALINOWSKI, K. MILCZAREK, J. SROKA, A. TOMASZEWSKI and J.A. WROTNIAK

Institute of Physics, University of Lodz, Lodz, Poland

K. MALUSZYNSKA and Z. WLODARCZYK

High Pedagogical School, Kielce, Poland

**M. AKASHI, M. AMENOMORI, E. KONISHI, H. NANJO and Z. WATANABE

Department of Physics, Hirosaki University, Aomori, Japan

K. MIZUTANI

Department of Physics, Saitama University, Saitama, Japan

K. KASAHARA, S. TORII and T. YUDA

Institute for Cosmic-Ray Research, University of Tokyo, Tokyo, Japan

T. SHIRAI, N. TATEYAMA and T. TAIRA

Faculty of Engineering, Kanagawa University, Yokohama, Japan

I. MITO

Shibaura Institute of Technology, Tokyo, Japan

M. SHIBATA

Faculty of Education, Yokohama National University, Yokohama, Japan

H. SUGIMOTO and K. TAIRA

Sagami Institute of Technology, Kanagawa, Japan

N. HOTTA

Department of Physics, Konan University, Kobe, Japan

***M. BALLESTER C. SANTOS, J. BELLANDI FILHO, J.A. CHINELLATO, C. DOBRIGKEIT, C.M.G. LATTES, A. MARQUES, M.J. MENON, C.E. NAVIA O., K. SAWAYANAGI, E. SILVA, E.H. SHIBUYA and A. TURTELLI Jr.

Instituto de Fisica Gleb Wataghin, Universidade Estadual de Campinas, Sao Paulo, Brazil

N.M. AMATO and F.M. OLIVEIRA CASTRO

Centro Brasileiro de Pesquisas Fisicas, Rio de Janeiro, RJ, Brazil

R.H.C. MALDONADO

Instituto de Fisica, Universidade Federal Fluminense, Niteroi, RJ, Brazil

H. AOKI, Y. FUJIMOTO, S. HASEGAWA, H. KUMANO, H. SEMBA, T. TABUKI, M. TAMADA, K. TANAKA and S. YAMASHITA

Science and Engineering Research Laboratory, Waseda University, Shinjuku, Tokyo, Japan

N. ARATA, T. SHIBATA and K. YOKOI

Department of Physics, Aoyama Gakuin University, Setagaya, Tokyo, Japan

A. OHSAWA

Institute for Cosmic-Ray Research, University of Tokyo, Tokyo, Japan

Received 9 March 1981
(Revised 23 June 1981)

Here we present a summary of joint discussions on the results of three mountain experiments with large-scale emulsion chambers, at Pamir, Mt. Fuji and Chacaltaya. Observations cover gamma quanta, hadrons and their clusters (called "families").

The following topics are covered, concerning the characteristics of nuclear interactions the energy region $10^{14}-10^{16}$ eV: (i) rapid dissipation seen in atmospheric diffusion of high-energy cosmic-rays; (ii) multiplicity and P_t increase in produced pi-mesons in the fragmentation region; (iii) existence of large-P_t jets, (iv) extremely hadron-rich family of the Centauro type; (v) exotic phenomena in the extremely high energy region beyond 10^{16} eV.

1. Introduction

During 1981, the first results of colliding proton and antiproton beams with particle energies of a few hundred GeV are expected to be obtained at CERN. Then, the days of the next generation of accelerators will soon come, with proton beam intersecting storage rings, which are planned to investigate the energy region up to 3000×3000 GeV^2.

Therefore, it is of interest to look at the cosmic-ray experimental data available at present, trying to see which kinds of new phenomena will be met in the concerned high energy region of $10^{14}-10^{16}$ eV in the laboratory system. This is also useful for planning future cosmic-ray experiments, which are bound to shift their working range towards higher particle energies. For this purpose, a symposium on high-energy cosmic-rays was held at Nakhodka, USSR, on 20–29 October, 1980.

The meeting was primarily devoted to the presentation of results from the three large-scale experiments using emulsion chambers exposed to cosmic-rays at mountain altitudes [1]; one at Pamir, Soviet-Poland Collaboration; one at Mt. Fuji, Japanese interuniversity Collaboration, and one at Chacaltaya, Brazil-Japan Collaboration. Comparison was made of the experimental results of the three, and there were further discussions on their comparison with information from other cosmic-ray experiments, such as those on underground cosmic-rays and on extensive air showers. As is known, in a number of investigations of extensive air showers, serious indications were obtained about an essential change of strong interaction features at super high energies [2]. The present article describes a summary of the results from the symposium with conclusions which were arrived at through joint discussions.

The emulsion chamber is an apparatus composed of a combination of photo-sensitive layers for the registration of showers (X-ray films and/or nuclear emulsion plates) and of material blocks for the generation of electron showers and for a nuclear interaction target. The simple chambers structure and the stability of the photo-sensitivity have allowed the performance of a cosmic-ray experiment with emulsion chambers of large area exposed over long periods at high mountain altitudes, yet keeping fine spatial resolution and good accuracy in shower energy measurements.

A brief description of the chambers and their exposure in the three mountain experiments is given in table 1 and fig. 1.

2. Gamma quanta and hadrons

Emulsion chambers can be classified into the following two categories: one of thin type and another of thick type, referring to the nuclear mean free path. The thin chamber records mostly electrons and gamma quanta (both will simply be called

TABLE 1
Mountain emulsion chamber experiments

Experiment	(altitude)	Atmospheric depth (g/cm^2)	Exposure ($m^2 \cdot$ year)	
			Thin-type	Thick-type
Chacaltaya	(5200 m)	540	281	225
Pamir	(4370 m)	594	1300	570
Mt. Fuji	(3750 m)	650	685	135

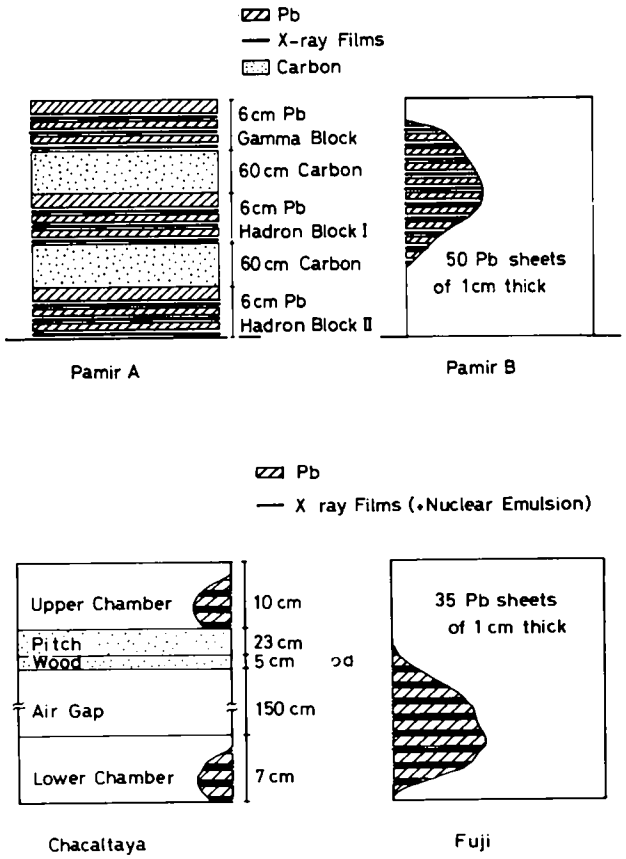

Fig. 1. Structure of typical emulsion chambers in Pamir, Mt. Fuji and Chacaltaya experiments.

gamma quanta, hereafter) arriving at the chamber from the atmosphere, while the thick chamber also observes hadrons, through their nuclear interactions in the chamber. The detection threshold for a shower, E_{thres}, is around 2–4 TeV, depending mostly on the type of X-ray film used in the chamber. This restricts the observation of gamma quanta with energy $E_\gamma \geq E_{\text{thres}}$, and hadrons with $E_h \geq E_{\text{thres}}/k_\gamma$, where k_γ expresses the gamma inelasticity, i.e., the fraction of energy released into gamma quanta in a nuclear interaction.

The information on observed gamma quanta and hadrons allows the determination of their fluxes, energy spectra and zenith angle distribution. The flux can be expressed as a function of energy, arrival direction and atmospheric depth of the observation station in the following way:

$$\frac{\mathrm{d}^2N}{\mathrm{d}E\mathrm{d}\Omega} = I\left(\frac{E}{E_{\text{thres}}}\right)^{-(\beta+1)} \exp(-t/\lambda_{\text{abs}}\cos\theta), \tag{1}$$

TABLE 2
Flux measurement on gamma quanta and hadrons

Experiment [reference]	Gamma-quanta		Hadrons		
	vertical flux with $E_\gamma \geq 3$ TeV ($m^{-2} \cdot yr^{-1} \cdot sr^{-1}$)	power in energy spectrum	vertical flux with $E_h^{(\gamma)} \geq 3$ TeV ($m^{-2} \cdot yr^{-1} \cdot sr^{-1}$)	power in energy spectrum	absorption mean free path (g/cm^2 in air)
Chacaltaya [3]	91 ± 10	2.05 ± 0.05	142 ± 9	1.80 ± 0.10	104 ± 4
Pamir [4]	60 ± 6	2.00 ± 0.05	96 ± 18	2.00 ± 0.10	103 ± 4
Mt. Fuji [5]	32 ± 5	2.00 ± 0.05	66 ± 10	1.80 ± 0.10	105 ± 5

where t expresses the atmospheric depth at the observational level, λ_{abs} is the mean free path for absorption and θ the zenith angle of arrival direction. For gamma quanta, E stands for E_γ, while, for hadrons, one is to replace E by $E_h^{(\gamma)} = k_\gamma E_h$.

Table 2 presents a summary of the results from the three experiments, Pamir, Fuji and Chacaltaya. The errors given are statistical only. Taking difficulties in the absolute calibration of energy measurement into account, the three sets of results are reasonably consistent.

Flux information on the cosmic-ray components in the atmosphere could be a useful source of knowledge of the characteristics of high-energy nuclear interactions, if we had accurate information on the primary cosmic-rays coming into the atmosphere. But, unfortunately, the only direct information at present available on the primaries is restricted to the lower energy region, and we have to rely on indirect estimation from various sources. Even with such ambiguities on the primaries, particularly their chemical composition, it can be made clear that the simple scaling model of nuclear interactions is ruled out under the assumption of normal composition. That is, if the known composition of primaries can be extended to higher energy regions of $\sim 10^{15}$ eV without a significant change, extrapolation of the scaling assumption of nuclear interactions predicts flux values of atmospheric gamma quanta five to ten times higher than the observed value. Thus, we find that the atmospheric diffusion of cosmic-rays must be accompanied by a more rapid dissipation than in the case of the above assumption.

Such an analysis can be extended into a still higher energy region $\sim 10^{16}$ eV, by observing the frequency of arrival of groups of high-energy cosmic-ray gamma quanta and hadrons. This phenomenon is called the "cosmic-ray family", the details of which will be discussed in the next section. Its comparison with the primary cosmic-ray intensity again shows a significant discrepancy in the case of the simple scaling assumption with primaries of normal composition. Thus, the above conclusion of rapid dissipation of high-energy cosmic-rays in the atmosphere applies up to the region of $\sim 10^{16}$ eV.

Simulation calculations were made extensively by a number of authors, covering various possibilities for the primary cosmic-rays and for the model of nuclear interactions [6]. It was found that a better fit is obtained by either of the following

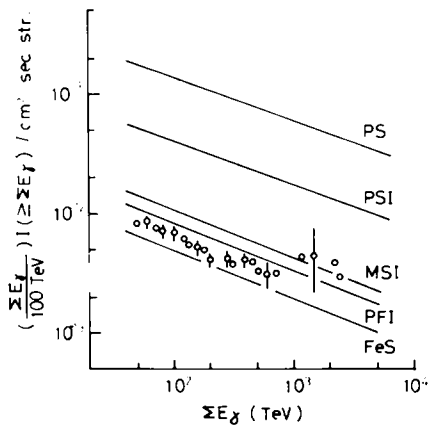

Fig. 2. Energy spectrum of gamma ray families ($E_{thres} = 2$ TeV) observed in the Mt. Fuji experiment. Simulation results by Kasahara, Torii and Yuda [6] are shown as follows: PS: proton scaling, PSI: proton scaling with increasing σ, PFI: proton fireball ($E_0^{1/4}$ law) with increasing σ, MSI: mixed primary composition scaling with increasing σ, FeS: iron primary scaling. Assumed power of primary spectrum: in proton case (P) and in iron case (Fe), -1.7; in mixed composition case (M), -1.8 for proton and alpha, -1.6 for L, M, H and -1.3 for Fe at $< 10^{15}$ eV and all -2.0 beyond. Absolute intensity is normalized to Grigorov's results.

assumptions or their combination: increase of the multiplicity, increase of the nuclear cross section and/or inelasticity, or increase of the heavy primary content, as the energy goes higher. A slow increase of the cross section has already been found in the present accelerator energy region, but its simple extrapolation has proved insufficient. Fig. 2 presents examples of such simulation analyses reported at the Nakhodka symposium.

3. Families of gamma quanta

The emulsion chamber often records a group of showers, parallel in their arrival direction and clustering in an area of small dimensions, often several cm and sometimes up to a few tens of cm. Such a group of showers is called a "family", because it shows the arrival of a bundle of high energy cosmic-ray gamma quanta and hadrons which have originated from one and the same primary particle. We will first discuss the average behaviour of families of gamma quanta (hereafter called gamma families) observed in emulsion chambers of both thin and thick types.

A family is a result of nuclear and electromagnetic cascade processes in the atmosphere originating from the arrival of a single primary particle. Therefore, the characteristics of high-energy nuclear interactions, which we are interested in, will be partly smeared out by the stochastic nature of the atmospheric processes. There are various approaches to high-energy physics studies through the observation of gamma families. Among these, extensive simulation calculations were carried out in several

laboratories covering wide varieties of nuclear interaction models [6]. Their results are useful not only for comparison with the experimental data but also for a better understanding of the family phenomenon.

It was noticed that higher energy gamma quanta in a family bring more direct information on the parent interaction than lower energy ones, because the electromagnetic cascade processes will be more dominant for gamma quanta with lower energy [7]. Thus the spectrum of fractional energy of gamma quanta, f', is constructed for each family, taking out lower energy ones in a way independent of family size. The quantity f' is defined as $f' = E_\gamma / \Sigma' E_\gamma$, where the summation Σ' is made over an energy interval with self-consistently defined lower limit $E'_{\min} = f'_{\min} \Sigma' E_\gamma$. Here, the value of $f'_{\min}$ is set at 0.04 for comparison of the three experiments. Fig. 3 presents the distribution of multiplicity n' of such gamma quanta with $f' \geq f_{\min}$ for families with $\Sigma' E_\gamma \geq 100$ TeV. Comparison with the simulation calculation shows that the scaling model is excluded. The experiment shows a larger frequency of high n' families. The models with a rapid multiplicity increase with energy, such as that with an $E_0^{1/4}$ law, give good agreement. This statement is also confirmed by fig. 4, where the mean value $\langle n' \rangle$ is presented at various intervals of family energy, $\Sigma' E_\gamma$, from the results of the Pamir and Fuji experiments, and compared with the results of simulation calculations made with various models.

Lateral spread of gamma quanta in a family is another quantity closely related to the parent nuclear interactions, because their observed spread is, in almost all cases, well above that expected from electron multiple scattering in atmospheric cascade processes and therefore its main part must be due to the angular spread in the nuclear interactions themselves. Fig. 5 presents the average lateral spread $\langle R_\gamma \rangle$ of gamma quanta in a family, at different intervals of family energy, ΣE_γ, from the

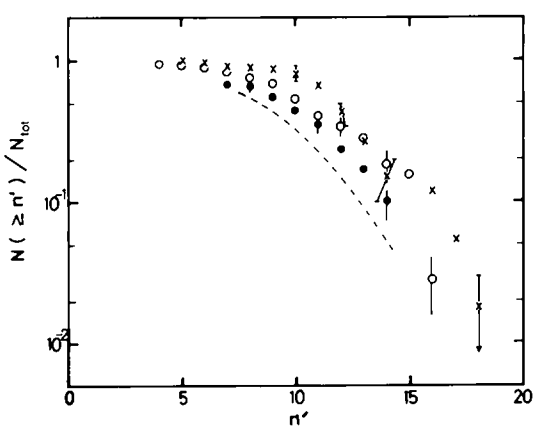

Fig. 3. Integral distribution of n', the multiplicity of gamma quanta with $f' > f'_{\min} = 0.04$, for families with $\Sigma' E_\gamma = 100 - 200$ TeV. ●: Pamir experiment, ×: Fuji experiment, ○: Chacaltaya experiment. The simulation result of the Pamir group [6] is shown by a broken line (scaling in the fragmentation region with increasing dissipation at $x \sim 0$, called the quasi-scaling model of FIAN, M4).

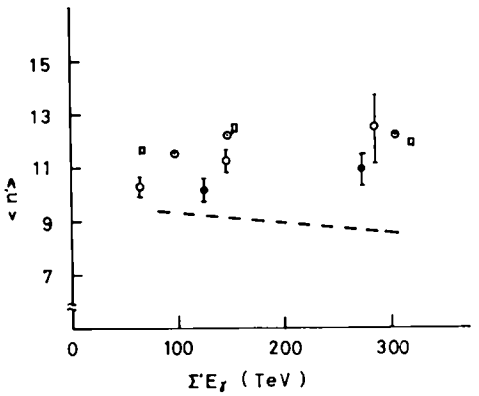

Fig. 4. Average value $\langle n' \rangle$ of the multiplicity ($f'_{min} = 0.04$) at different family energies, $\Sigma' E_\gamma$. ●: Pamir experiment, ○: Fuji experiment. The simulation results are shown as, ⊙: SH of Pamir (heavy fireball), □: PFI of Fuji (proton fireball with increasing σ), dashed line: M4 of Pamir (quasi-scaling).

Pamir and Fuji experiments. Here again, the scaling model is ruled out, since the scaling simulation calculation gives too small an average lateral spread. If we want to interpret the observed large spread by the increase of P_t alone, the average value $\langle P_t \rangle$ in the nuclear interaction has to be made as large as twice the value in the accelerator energy region. It should be pointed out here that increase of both multiplicity and heavy primary content have the same effect of increasing the lateral spread, because, for a fixed ΣE_γ, both lead to smaller effective energies of gamma quanta at their birth in the parent interaction.

Now we know that every average aspect of gamma families – the energy distribution and the lateral spread of gamma quanta – confirms the previous conclusion of rapid dissipation in atmospheric diffusion of high-energy cosmic-rays. Furthermore, they show that such rapid dissipation can not just be due to an increase of cross section or inelasticity, and that we cannot do without the rapid multiplicity enhance-

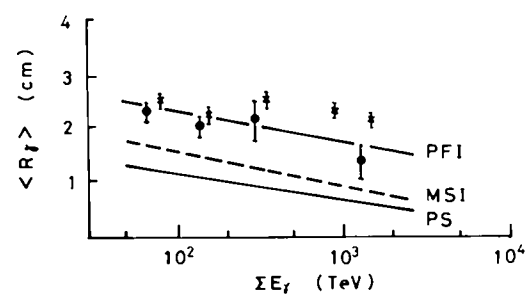

Fig. 5. Average lateral spread of gamma quanta with $E_{thres} = 4$ TeV in a family ($N_\gamma > 4$) at different intervals of ΣE_γ. ●: Fuji experiment, ×: Pamir experiment. Simulation results of the Mt. Fuji group are shown for comparison. $\langle P_{t\pi} \rangle$ is 330 MeV/c for the scaling case (PS and MSI) and 400 MeV/c for the fireball case (PFI).

ment taking place in the foremost region of the jets, i.e., the so-called fragmentation region. In other words, the energy distribution (x-distribution) of secondary hadrons is becoming softer. If we assume an increase of multiplicity such as one with the traditional $E_0^{1/4}$ law, then the lateral spread necessitates a slow increase of the average P_t of produced secondary pions.

The above conclusion of broken scaling is based on the assumption that the chemical composition of primary cosmic-rays undergoes no significant change up to the concerned high-energy regions. An increase in the content of heavy nuclei among the primary particles, if it exists, gives almost the same effect on the families as an increase of pion multiplicity in hadronic interactions. We may visualize that a primary heavy nucleus of mass number A will behave approximately equivalent to an incoming bundle of A nucleons. In fact, the simulation calculations show that differences between the two alternatives can hardly be seen in the average behaviour of gamma families hitherto studied.

It is pointed out that such broken scaling in the nuclear interaction seen from family study is in agreement with the result of the Chacaltaya emulsion chamber experiment on target nuclear interactions [8a]*. The study of these target nuclear interactions, though covering a lower energy region of $\Sigma E_\gamma = 20-100$ TeV, is free from ambiguities inherent in the studies of atmospheric cosmic-ray phenomena such as the gamma-families. There it was found that half of the interactions are just on the scaling extrapolation of those in the accelerator energy region, while the other half have significantly larger multiplicity and increased P_t. The average behaviour over all the events follows along the $E_0^{1/4}$ law of increase of multiplicity.

Thus, the above characteristics found in the gamma families are connected to broken scaling characteristics of the nuclear interaction itself in the energy region of $\sim 10^{15}$ eV.

4. Decascading and jet analysis

It is an ideal in a study of gamma families to reconstruct the original atmospheric nuclear interactions themselves. The first step towards the ideal is the procedure called "decascading", which intends to trace back the atmospheric cascade processes for reconstruction of the original gamma quanta at the point of their production [9, 8]. In gamma-ray families, we are able to recognize such local clusters of gamma quanta as those from the atmospheric cascade processes.

* After completion of the original manuscript, the authors were informed of the latest simulation calculation publication by Ellsworth, Gaisser and Yodh on target nuclear interactions [8b]. Here, they found reasonable agreement on the average distributions of gamma quanta with the Chacaltaya experimental data, if the two components (normal P_t and high P_t) are introduced for the produced pions. Their introduction of the high-P_t component yields an increase of average P_t as well as of gamma quanta multiplicity in the rapidity scale.

The decascading procedure commonly adopted in the three experiments is to use the parameter z_{ik} between ith and kth gamma quanta in a family, defined as

$$z_{ik} = E_i E_k R_{ik} / (E_i + E_k), \tag{2}$$

where E_i and E_k are the respective energies and R_{ik} their mutual distance. If $z_{ik} < K$, the quantum pair is decascaded into a single quantum with energy $E_i + E_k$ at the position of the energy center of the two. Repeating the process of joining the two over all possible pairs of quanta, we arrive at the "decascaded" family where every pair of quanta satisfies the condition $z_{i'k'} > K$, meaning that between no pair of quanta does there exist any kinship through the atmospheric electromagnetic cascade processes. The numerical value of K in the criterion is chosen as 10, 11 and 12 TeV·mm at Fuji, Pamir and Chacaltaya, respectively.

The decascaded family gives us the configuration of original gamma quanta at the point of production, though their energies E^* do not give their initial value at the parent interaction and no information is yet available on the height of their production. (Quantities referring to the decascaded quanta are expressed with an asterisk.) It has been shown that the product E^*R^* of the decascaded quanta is approximately proportional to P_t at the parent interaction, irrespective of the height of interaction [9, 8]. This approximate rule holds over a wide range of height, unless the interaction happens very near the chamber ($\gtrsim 500$ m) or very far away ($\gtrsim 5$ km). Fig. 6 gives the diagram of E^* versus R^* for every decascaded gamma quantum, R^* being the distance from the family center. Also shown is the E-R diagram of gamma quanta in the target interaction from the Chacaltaya experiments, where the distance to the production point is fixed and, moreover, the decascading procedure is not necessary [8]. Their comparison confirms the above approximate relation on E^*R^*, and makes it possible to fix the proportionality constant at $P_t(\gamma) \sim E^*R^*/1$ km, meaning that the effective height of production is about 1 km.

What is remarkable about the decascaded family is that we often see the cluster structure even after the decascading procedure. Such a cluster structure cannot be attributed to the electromagnetic cascade processes, but the origin must be looked for in the nuclear interaction. Anticipating them to be high-P_t jets seen in accelerator experiments, for example, the following procedure is applied commonly to the data of the three experiments. We construct z^*_{ik} defined as in (2) on a pair of the decascaded gamma quanta, ith and kth, and impose the criterion $z^*_{ik} < K^*$, for putting the pair jointly into one. Repeating the procedure over all possible combinations of pairs, we finally arrive at a family composed of jets. The value of K^* in the criterion is set as 200, 220 and 240 TeV·mm, for the three respective experiments. Since the effective production height is about 1 km, the above value amounts to assuming that the P_t of gamma quanta perpendicular to the jet axis is $\lesssim 240$ MeV/c.

Fig. 7 presents the diagram of $E^{(\gamma)}_{\mathrm{jet}}$ and R_{jet}, the gamma quanta energy sum and the distance from the family center of all jets reconstructed by applying the above

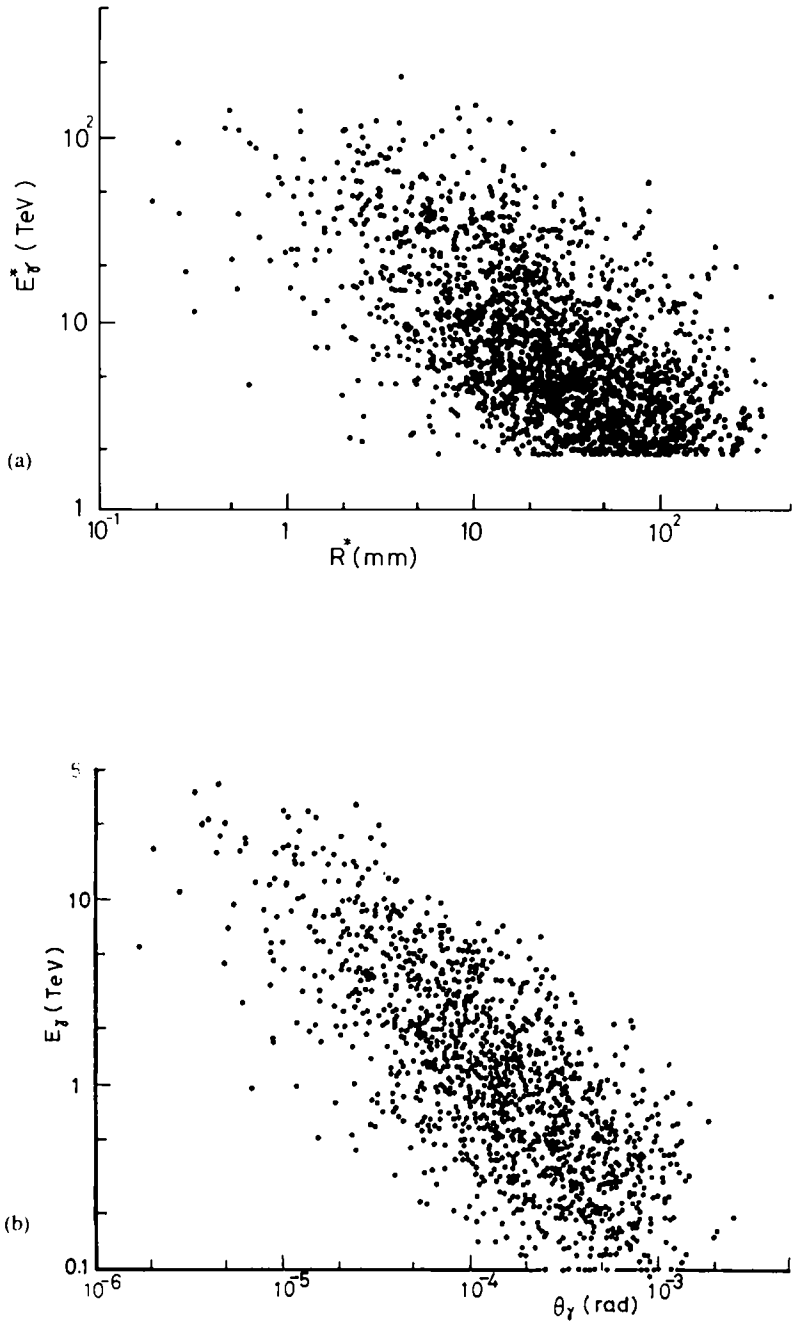

Fig. 6. (a) Diagram of E^*, energy, versus R^*, distance from the center, of all the decascaded gamma quanta in families with $\Sigma E_\gamma > 100$ TeV. Data are from Chacaltaya experiment. (b) Diagram of E_γ, energy, versus θ_γ, emission angle for all gamma quanta in target interactions ($\Sigma E_\gamma > 20$ TeV), for the Chacaltaya experiment.

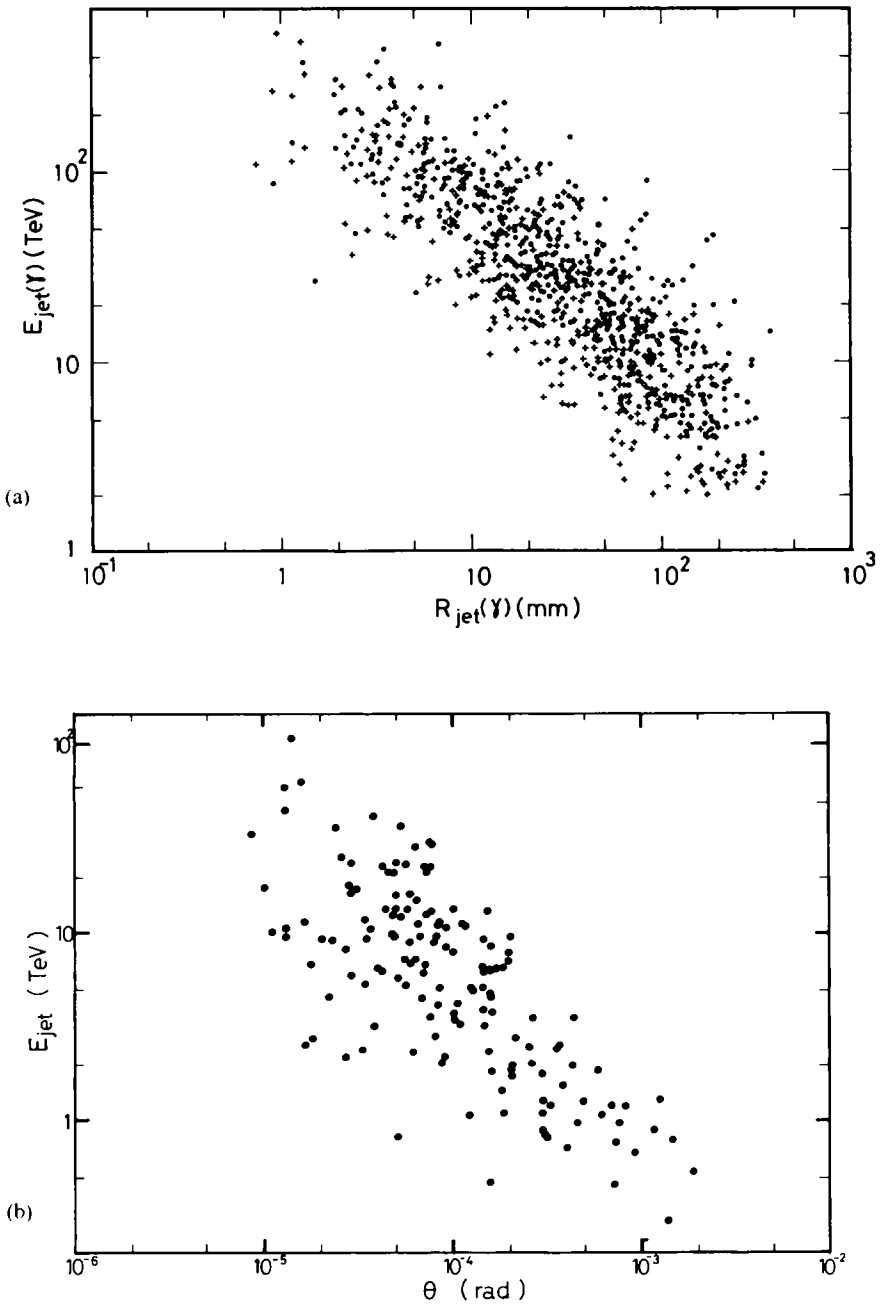

Fig. 7. (a) Diagram of energy, $E_{jet}^{(\gamma)}$, versus distance from the center, R_{jet}, for all reconstructed jets in the gamma families with $\Sigma E_\gamma > 100$ TeV. +: Fuji experiment, ●: Chacaltaya experiment. (b) Diagram of energy, E_{jet}, versus emission angle, θ_γ, for all the reconstructed jets in the target interactions ($\Sigma E_\gamma > 20$ TeV) for the Chacaltaya experiment.

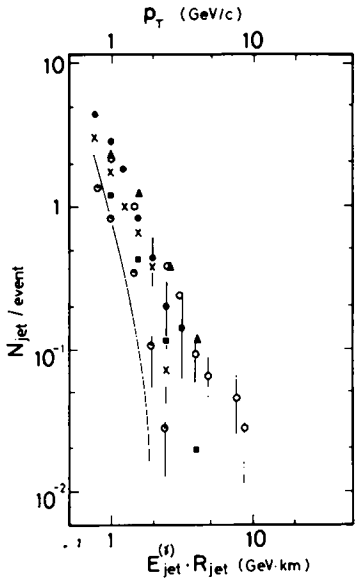

Fig. 8. Integral spectrum of $E^{(\gamma)}_{jet} \cdot R_{jet}$ of jets in families with $\Sigma E_\gamma > 100$ TeV. Pamir experiment: ■ ($\Sigma E_\gamma = 100 \sim 200$ TeV), ▲ ($\Sigma E_\gamma = 200 \sim 500$ TeV); Fuji experiment: × ($\Sigma E_\gamma = 100 \sim 200$ TeV), ● ($\Sigma E_\gamma = 200 \sim 500$ TeV); Chacaltaya experiment: ○ ($\Sigma E_\gamma > 100$ TeV). Results of $P_t^{(\gamma)}$ (jet) from target interactions ($\Sigma E > 20$ TeV) are presented by ⊙. The two scales on the abscissa, i.e., $E^{(\gamma)}_{jet} \cdot R_{jet}$ and $P_t^{(\gamma)}$ (jet), are normalized to each other, taking the effective production height as 1 km. The simulation results of the Mt. Fuji group with scaling assumptions on gamma families are presented together by the solid line.

procedure on gamma families with $\Sigma E_\gamma \geqslant 100$ TeV. For comparison, the result of jet analysis on the target interactions is also presented. Fig. 8 shows the spectrum of the product $E^{(\gamma)}_{jet} R_{jet}$ for the same set of gamma families, together with that for target interactions. It is seen that the $E^{(\gamma)}_{jet} R_{jet}$ distribution for gamma families extends towards higher ER region, while that for the target interactions has a sharp drop.

Jets with large ER in gamma families are unambiguous clusters of showers located far away from the family center, and one can think of the following possibilities of their origin. One is production of high-P_t jets in nuclear interactions, the existence of which has been already known in the present accelerator region. The transverse momentum of a jet, P_t(jet), can be approximately estimated as,

$$P_t(\text{jet}) \sim E^{(\gamma)}_{jet} R_{jet} / k_\gamma(\text{jet}) \cdot 1 \text{ km}. \tag{3}$$

Here, the effective production of height is ~ 1 km, where k_γ(jet) expresses the fraction of energy of a jet given to gamma quanta, in a similar way as the gamma inelasticity k_γ does for the nuclear interaction case. One sees that the high-P_t jets, found particularly in gamma families but not in target interactions, are those with $P_t(\text{jet}) \gtrsim 5$ GeV/c, assuming $k_\gamma(\text{jet}) \sim 0.5$. Though the distribution approximately

follows $P_t dP_t/P_t^4$, one should notice that their frequency of occurrence, i.e., 0.38 ± 0.08 per family, is much higher than found from accelerator and target interaction experiments. For the target interactions, Shibata analysed their high-P_t gamma quanta and found the frequencies to be consistent with expected values from the model of hard scattering between subhadronic constituents [10].

Another possibility is that a cluster of showers with large ER comes from an atmospheric interaction of a secondary hadron with a long path in the atmosphere after its production. The case is studied by simulation calculation and the results are shown in fig. 8. It is seen that simulation with ordinary nuclear interaction models gives less frequency to the high-ER jets and some extra source of high-P_t hadrons will be necessary for interpretation of the experimental results.

5. Binocular families

The existence of a large-P_t jet in gamma families was first noticed through the observation of families of "binocular" type, i.e., those consisting of two distinct clusters with a large distance between them [11]. Fig. 9 presents typical examples of such binocular families. The probability of a chance coincidence, i.e., that of two independent families being mistaken as a binocular family, depends on the accuracy of the direction measurements of the events, but it generally turns out, for $\Sigma E_\gamma \gtrsim 100$ TeV, to be of the order of 10^{-3} of all the gamma families, which is significantly smaller than the actual observed rate of binocular ones, i.e., several percent of the whole.

It is clear just from visual observation that the binocular families will have large P_t(jet) between the two constituent clusters. One may then ask, inversely, whether or not families with large P_t(jet) are of binocular type. Results of the jet analysis of gamma families, described in the previous section, can give an answer. It is found that, among families with high P_t(jet), about half are of binocular type with $N_{jet} = 2$, while the rest have large N_{jet}. N_{jet} expresses number of jets in a family defined by the procedure of the previous section. Thus, the binocular families ($N_{jet} = 2$) can be considered, in fact, as a specific type of family, reflecting some particular type of parent nuclear interactions. At the same time, one notices that the families with very large N_{jet} are almost always associated with high-P_t jets.

The same conclusion can be arrived at by the analysis of the azimuthal asymmetry of gamma families made by the Pamir group [12]. They introduce a parameter α, for describing the asymmetry, with the following definition,

$$\alpha = \left(\sum_{i \neq j} \cos 2\varepsilon_{ij} \right) \Big/ n_\gamma (n_\gamma - 1). \tag{4}$$

ε_{ij} is the azimuthal angle between the ith and jth gamma quantum in a family. The summation here runs over all possible combinations of pairs in a family. With such a

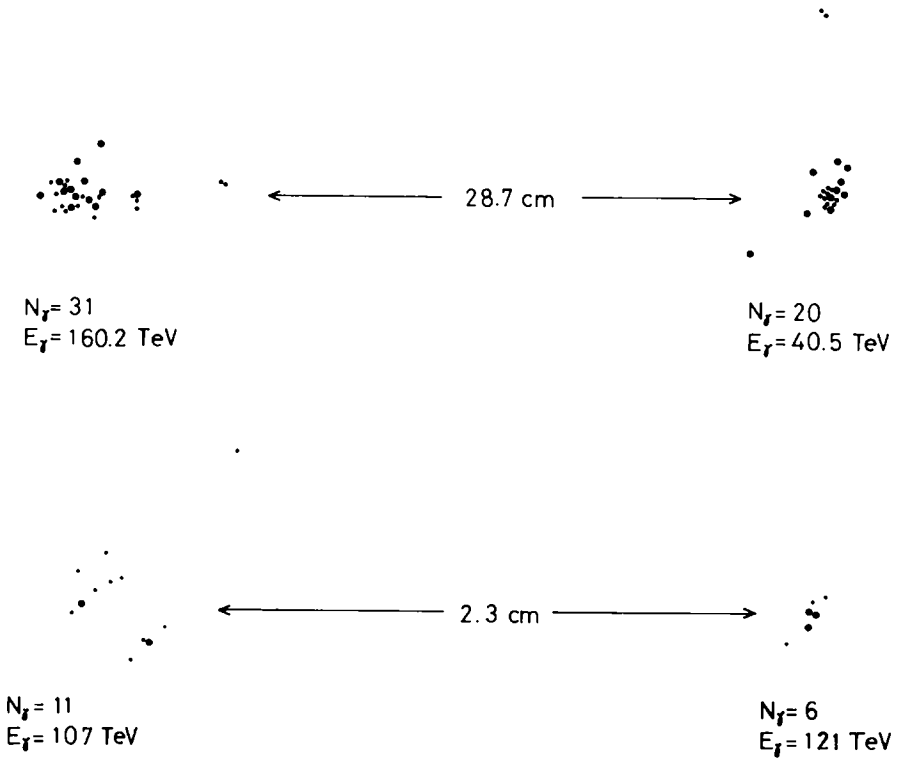

Fig. 9. Examples of target maps of binocular families. (a) one from Chacaltaya experiment (event # 16-S180); (b) one from Pamir experiment (event no. 1714).

definition, the case with $\alpha = 0$ corresponds to complete isotropy, while $\alpha = 1$ gives the opposite extreme case of coplanar families. Fig. 10 presents the average $\langle\alpha\rangle$ of observed families in different energy intervals and also of the simulated ones in the corresponding energy intervals. It is seen from comparison that the large multiplicity model, such as the HS model of the Pamir group, gives too small an $\langle\alpha\rangle$, though the same model has already been found to give an over-all agreement on other average aspects of families. Thus, one now knows that families with large azimuthal anisotropy constitute a certain fraction of events, and they are of a type outside the currently adopted model of nuclear interactions. It is the low-N_{jet}, high-P_t families that constitute such anisotropic families.

Further detailed study is made of the binocular families with increased statistics, applying the following common criteria for selection of the binocular type events:

(i) $\Sigma E_\gamma > 100$ TeV, E_1 and $E_2 > 10$ TeV and $E_1 + E_2 > 0.8\ \Sigma E_\gamma$, where E_1 and E_2 are the energy of the first and second cluster in a family;

(ii) $R_{12} > 5(\langle r\rangle_1$ and $\langle r\rangle_2)$, where $\langle r\rangle_1$ and $\langle r\rangle_2$ are the average lateral spread for the first and second cluster and R_{12} is the distance between the two clusters.

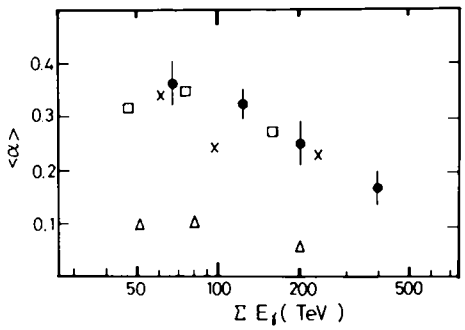

Fig. 10. Average value of anisotropy parameter $\langle\alpha\rangle$ for gamma families of different ΣE_γ intervals. Pamir experiment: ●, Pamir simulation: × for scaling (S), □ for scaling with doubled P_t (NS) and △ for heavy fireball (HS).

Fig. 11 presents the frequency of binocular families defined in this way, where the distance between the two clusters is expressed by the energy-normalized quantity, representing their two-body gamma-ray invariant mass times the production height, $\chi_{12} = R_{12}(E_1 E_2)^{1/2}$. The results are compared with the simulation results.

An interpretation of such binocular families was presented by the Chacaltaya group [11]. They proposed the production of a hypothetical particle "geminion" in the parent interaction, which decays into two particles (hadrons but not pi-mesons) with Q-value as large as 20–30 GeV. Here, two particles of the decay product are considered to be responsible for clusters of binocular families.

6. Hadron families and their accompanied gamma quanta

One of sensations of the Chacaltaya experiment is the discovery of families of extreme composition, called Centauro and Mini-Centauro, rich in hadrons and poor

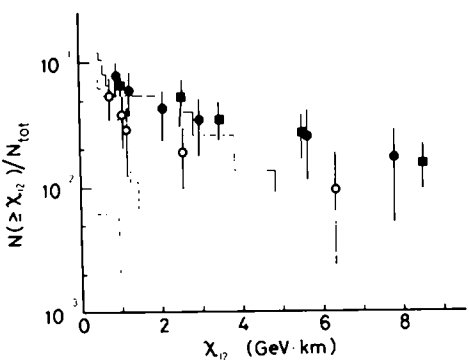

Fig. 11. χ_{12} distribution for binocular families. For the definition of χ_{12} and the selection criteria for binocular families, see text. ■: Pamir experiment, ○: Fuji experiment, ●: Chacaltaya experiment. The simulation results of Fuji group are presented together. Full curve, MSI; dashed curve, PS; dot-dashed curve, PF.

TABLE 3
Scanning results for Centauro-type families: Criteria[a]: (i) $\Sigma E_\gamma + \Sigma E_h^{(\gamma)} \geq 100$ TeV; (ii) $N_h > 30$; (iii) $N_h > N_\gamma$

Experiment	Altitude (g/cm^2)	Total exposure of thick-type chamber ($m^2 \cdot$ year)	Number of Centauro	
			expected[b]	observed
Chacaltaya	540	200		5
Pamir	596	600	6	1
Mt. Fuji	650	135	1–2	1

[a] N_h is after the correction for detection loss.
[b] Expected values are derived from Chacaltaya data.

in gamma quanta [13]. The families called Centauro are interpreted by them as from a parent interaction with the emission of about one hundred hadrons without any accompaniment of gamma quanta (neutral pi-mesons). Events containing a smaller number of hadrons, almost without gamma quanta, were called Mini-Centauro.

The first question is whether families with such extreme composition have been observed in other mountain experiments with comparable frequency. Table 3 presents a summary of experimental situation for the three experiments in the search of hadron-rich families. Fig. 12 shows the diagram of number of gamma-quanta, N_γ, and of hadrons, N_h, for observed families in the three experiments. Here, the number of hadrons, N_h, is the estimated number of hadrons arriving at the chamber after applying corrections for detection efficiency, which varies from one chamber to

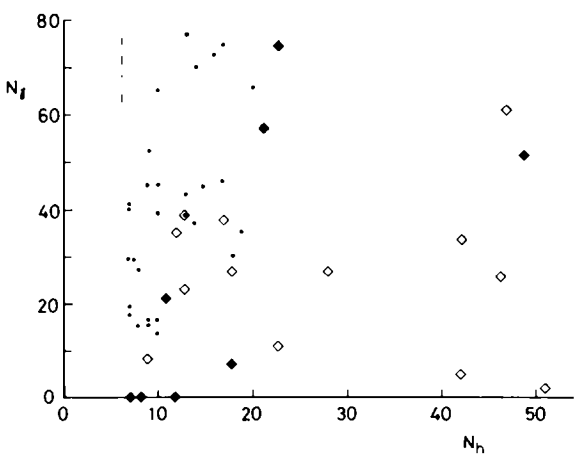

Fig. 12. Diagram of number of gamma quanta, N_γ, and of hadrons, N_h, for families with $\Sigma(E_\gamma + E_h^{(\gamma)}) > 100$ TeV. ◇: Centauro and Mini-Centauro of the Chacaltaya experiment; ◆: events of the same type of the Pamir experiment. Simulation events of the Pamir group, with the assumption of normal pion production and proton primary, are presented by small dots.

another. It is seen that there are families of extreme composition and, in particular, one Pamir experiment shows hadron-rich composition comparable to Chacaltaya's Centauro.

The next question is, of course, whether events with such an extreme composition as Centauro and Mini-Centauro can be attributed to trivial fluctuation in the nuclear cascade processes in the atmosphere. To check this, simulation calculations were carried out by several laboratories with various models of nuclear interaction and primary composition [5, 14]. The results with proton primary are presented in fig. 12. It can be seen that the Centauro-type events are located far from the simulated events and have to be attributed to some new process of nuclear interaction. Meanwhile, the Mini-Centauro events can be reproduced by the simulation calculation based on ordinary assumptions of nuclear interactions, as far as one is concerned with their distribution in the diagram of fig. 12.

It was suggested that the hadron/gamma quanta abundance in a family has to be studied not only as reflected by their particle number but also by the energy fractions carried by them. Fig. 13 presents one such improved diagram, where the number of hadrons, N_h, and the energy fraction in the hadron component, $\Sigma E_h^{(\gamma)}/\Sigma(E_h^{(\gamma)} + E_\gamma)$, are used as the parameters. The simulation calculation shows that fluctuation in nuclear cascade processes can only rarely generate a family with high values for the two parameters at the same time. It is possible to have a hadron-energy-rich family by fluctuation. In this family, however, a large part of the energy flow is in general carried by the surviving nucleon and therefore the hadron number is small.

The Chacaltaya group reported two new events of Mini-Centauro type, both of which were fortunate enough to allow a geometrical measurement on the height of parent interaction in the atmosphere. In both events distances between the shower cores are measured in both the upper and lower chambers, located a vertical distance of 180 cm from each other. The divergence of arrival direction between several pairs of penetrating shower cores comes out to be beyond the experimental error, and the results give 300 ± 100 m for event #139S-105I in chamber no. 19 and 160 ± 30 m for event #18S-18I in chamber no. 12 as the estimated height of their parent interaction. Some description of the events is given in table 4. They give new support to the existence of Mini-Centauro as a new type of nuclear interaction, and at the same time give a definite knowledge of the P_t of hadrons produced in the interaction. The average value of P_t for hadrons comes out as $P_{t,h}^{(\gamma)} = 0.35 \pm 0.1$ GeV/c, in agreement with that observed for the event Centauro I by the same geometrical method.

7. Exotic events of very high energy

There were reported a number of exotic events which suggest the existence of new phenomena in the extremely high energy region beyond 10^{15} eV. Of these, a short

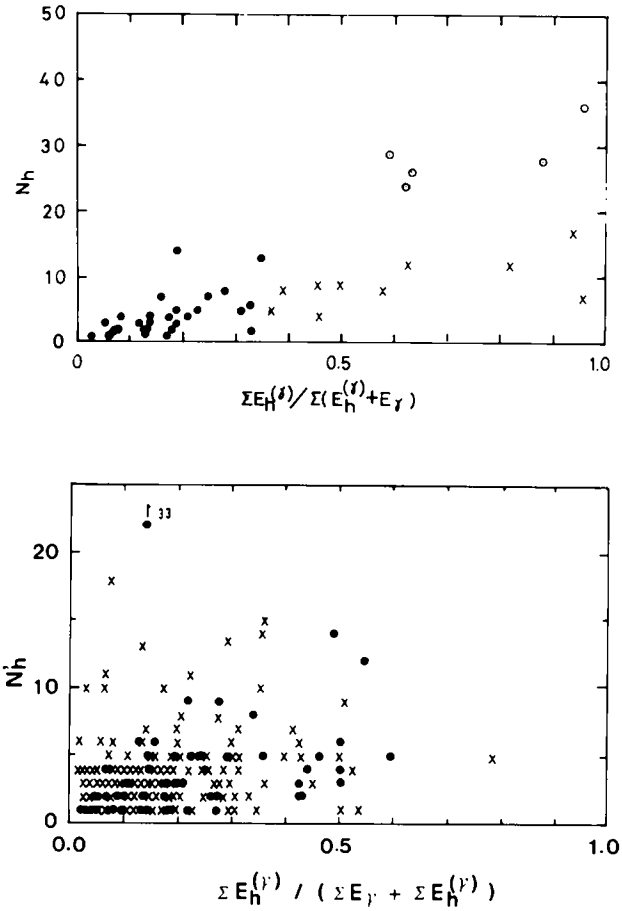

Fig. 13. Diagram of number of hadrons N_h and the energy fraction of hadron components, $\Sigma E_h^{(\gamma)}/\Sigma(E_h^{(\gamma)} + E_\gamma)$. (a) Chacaltaya experiment (families with $\Sigma(E_h^{(\gamma)} + E_\gamma) > 100$ TeV. ○: Centauro type, ×: Mini-Centauro type, ●: others. (b) Fuji experiments. ●: observed families with $\Sigma(E_h^{(\gamma)} + E_\gamma) >$ 50 GeV and $N_\gamma \geq 4$, ×: simulation MSI. N_h' expresses the number of nuclear interactions located between 6 and 22 c.u. of depth in the chamber.

description will be presented for the two events, "Tatyana" of the Pamir experiment [15] and "Titan" of Fuji experiment [16], because of their distinct character.

Tatyana, Pamir experiment, has a total visible energy of more than 13000 TeV, meaning that it is one of the highest energy events observed so far in emulsion chambers. The event was recorded by the thick chamber consisting of a gamma-layer and four hadron layers with carbon block, the total thickness of the chamber being 26 cm Pb plus 320 cm carbon, i.e., nearly 5 nuclear mean free paths or 55 radiation units. As is seen in fig. 14, what is remarkable here is that there is a penetrating black core with halo all through the chamber. The energy estimation of the core with

TABLE 4
Two new events of Mini-Centauro type, Chacaltaya experiment

Shower no.	E (TeV)	$P_t^{(\gamma)}$ (GeV/c)	Remark
(A) Event #139S-105I in chamber no. 19			
#1	14.9	0.49	A-jet
#2	6.8	0.14	Pb-jet-upper
#3*	18.0	0.16	A-jet
#4	21.6	0.23	A-jet
#5*	16.0	0.34	Pb-jet-upper
#6*	11.1	0.45	Pb-jet-upper
#7	8.0	0.50	A-jet
#8 ~ #15	14.0	0.79	A-jet
(B) Event #18S-18I in chamber no. 12			
Shower no.	E (TeV)	P_t (GeV/c)	Remark
#1*	3.3	0.17	Pb-jet-upper
#2	67.0	0.48	Pb-jet-upper
#3*	40.0	0.16	Pb-jet-upper
#4	14.0	0.22	Pb-jet-upper
#5	20.0	0.51	Pb-jet-upper
#6	18.0	0.38	Pb-jet-upper
#7	20.0	0.36	Pb-jet-upper
#8	80.0	0.25	C-jet
#9	14.0	0.18	C-jet
#10	5.0	0.035	Pb-jet-upper
#11	20.0	0.13	Pb-jet-lower
#12	2.0	0.063	Unidentified
#13	14.0	0.22	Unidentified
#14	2.3	0.073	Unidentified
#15	9.5	0.38	Unidentified
#16	3.5	0.21	Pb-jet-upper
#17	3.8	0.17	Unidentified
#18	3.1	0.13	Unidentified
#3′	17.0	0.063	Pb-jet-lower

Showers with an asterisk have a collimated core both in the upper and the lower chamber and are used for the geometry measurement.

halo is carried out by integrating the darkness in X-ray films, and it gives 8000 TeV. This is a lower limit, because the blackness of the core does not show any sign of attenuation down to the bottom of the chamber, so that a considerable fraction of the energy must have been lost in penetrating such large thickness. Outside the region of core with halo, of diameter of about 1 cm, there are numerous showers. Altogether, there are 224 gamma quanta with $\Sigma E_\gamma \sim 3200$ TeV and 66 hadrons with $\Sigma E_h^{(\gamma)} \sim 1500$ TeV in the peripheral region.

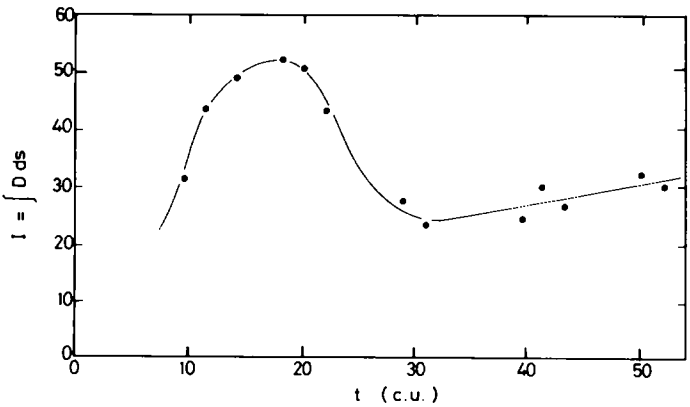

Fig. 14. "Tatyana" of the Pamir experiment with penetrating black core. The curve presents the variation of total darkness of the core with halo in the X-ray films with depth in radiation unit in the chamber.

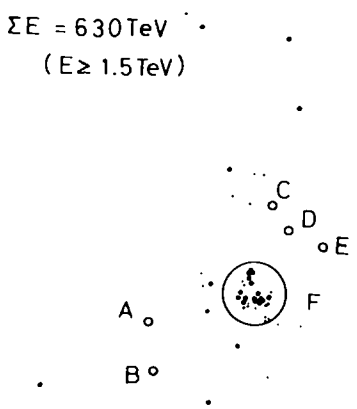

Fig. 15. Target diagram of the event "Titan" of the Fuji experiment. Showers of large energy are listed below.

Shower	Visible energy (TeV)	$k_\gamma P_t^{a)}$ (GeV/c)	Remarks
A	91	1.1	hadron
B	119	1.8	hadron
C	43	0.5	hadron
D	164	2.1	can be hadron
E	52	0.8	can be hadron
F (cluster)	130	0.5	can be A-jet

[a)]Production height $H = 1$ km is assumed for estimation.

TABLE 5
Hadron-rich family with large P_t

Event #198S-154I in the chamber no. 19			
Shower no.	E (TeV)	P_t (GeV/c)	Remark
1*	90.0	4.57	Pb-jet-upper
2	13.7	0.80	Pb-jet-upper
3	13.0	0.95	Pb-jet-upper
4	17.2	1.21	Pb-jet-upper
5	4.7	0.44	Pb-jet-upper
6	2.9	0.31	Pb-jet-upper
7	10.6	0.59	A-jet
8*	70.0	1.46	Pb-jet-upper
9	13.8	0.74	Pb-jet-upper
10	35.4	1.27	A-jet
11	28.6	2.65	A-jet
12*	14.2	1.20	A-jet
13	38.1	3.81	A-jet
14	4.0	0.48	Pb-jet-upper
15	12.5	0.77	C-jet

Showers with an asterisk have a collimated core both in the upper and lower chamber and are used for the geometry measurement.

Because of the penetrating power, a large part of the central core with halo must be composed of hadrons, but with no electromagnetic component. The double maximum structure of the shower transition curve and existence of subcores in the lateral structure suggest that the central core is composed of a bundle of collimated hadrons, at least three of comparable energy.

It is interesting to make a comparison with the event "Andromeda" of the Chacaltaya experiment, which is also one of the highest energy events so far observed. Here, we recognize a large black core with halo at the center, the total energy of which is estimated as about 20000 TeV. But the core with halo here shows steady attenuation in the chamber, so that it is interpreted as caused by a bundle of high-energy atmospheric gamma quanta of very large number. Observation of the hadron component is approximate because the chamber contained only 18 cm Pb without carbon blocks. After correction for the detection efficiency, the observed hadron energy flow is estimated as $\Sigma E_h^{(\gamma)} \sim 4000$ TeV.

Thus, one sees that the two, Tatyana and Andromeda, have quite different composition, i.e., Tatyana is rich in hadrons and Andromeda is rich in gamma quanta, though the two are with comparable energy beyond 10^{16} eV.

Titan, Fuji experiment, was observed by a thick chamber of solid Pb block of 40 cm thickness. As is seen in fig. 15, the main part of Titan consists of a few very high energy hadrons. As is stated in the caption, it is possible that all the secondaries are hadrons at the point of their production. As is stressed by the authors, a remarkable

characteristic of the event is its large P_t. P_t estimation is given in the caption assuming the production height to be about 1 km, and the average value turns out to be $\langle P_{t,h}^{(\gamma)} \rangle \sim 1.1$ GeV/c. The value can very well be an underestimate, because survival of a large fraction of secondary hadrons without atmospheric interaction makes it more plausible that the height of production is less than one mean free path, i.e., 1 km of atmosphere.

Recently, there was found one event from Chacaltaya, which shows hadron production with such large P_t. It is the event named #198S-154I in chamber no. 19 observed in the two-storey chamber with carbon target. As is seen in table 5 for summary of the event, the family is as rich in hadron content as Centauro or Mini-Centauro. Since the event penetrated through both the upper and lower chambers, we were able to apply the geometrical measurement of the arrival directions of the penetrating showers, and the result gives a production height estimate as 330 ± 30 m above the chamber. This allows estimation of P_t for the observed secondaries, as is seen in the table. The average value turns out to be $\langle P_{t,h}^{(\gamma)} \rangle \sim 1.42$ GeV/c, a lower bound from the energy measurement for penetrating showers, of the same order of magnitude as of Titan.

Thus, the parent interaction of these events cannot be Mini-Centauro, but their experimental data suggest the existence of some new species of nuclear interaction.

References

[1] Pamir experiment:
Acta Univ. Lodz ser. II, no. 60 (1977), 13th Int. Cosmic-ray Conf. (1973) vol. 3, p. 2228; 14th Int. Cosmic-Ray Conf. (1975) vol. 7, p. 2365
Mt. Fuji experiment:
AIP Conf. Proc. no. 49 (1979) 334; 16th Int. Cosmic-ray Conf. (1979) vol. 6, p. 344; vol. 7, pp. 68, 284, 294; vol. 13, pp. 87, 92, 98
Chacaltaya experiment:
AIP Conf. Proc. no. 49 (1979) 94, 145 and 317; 16th Int. Cosmic-ray Conf. (1979) vol. 6, pp. 350, 356, 362

[2] S.J. Nikolsky, Proc. 9th Int. High-energy Symp., Tobor, CSSR 21 (1978);
S. Miyake, Proc. 19th Int. Conf. on High-energy physics (1978) 433;
S.N. Vernov, Physica 3 (1977) 1601;
G.B. Khristiansen, JETP Lett. 28 (1978) 124

[3] Brazil-Japan Emulsion Chamber Collaboration, 13th Int. Cosmic-ray Conf. (1973) vol. 3, p. 2219

[4] Pamir Collaboration, Izv. Acad. Nauk USSR, ser. Phys. 38 (1974) 918; 14th Int. Cosmic-ray Conf. (1975) vol. 7, p. 2365

[5] Mt. Fuji Emulsion Chamber Group, 16th Int. Cosmic-ray Conf. (1979) vol. 7, p. 68

[6] Pamir experiment:
A.M. Dunaevsky, A.V. Urysson, Yu.A. Emelyanov, B.F. Shorin and M.A. Tashimov, FIAN preprint no. 150 (1975); Acta Univ. Lodz ser. II, no. 60 (1979) 199
I.P. Ivanenko, B.P. Kanevsky and T.M. Roganova, JETP Lett. 40 (1978) 704; 16th Int. Cosmic-ray Conf. (1979) vol. 7, pp. 101, 198;
J.A. Wrotniak, Acta Univ. Lodz ser. II, no. 60 (1977) 165;
A. Krys, A. Tomaszevski and J. Wrotniak, 16th Int. Cosmic-ray Conf. (1979) vol. 7, pp. 182, 186;
Y.A. Fomin, J. Kempa, G.B. Khristiansen, T.G. Levina, A. Piotrowska and J. Wdowczyk, 15th Int. Cosmic-ray Conf. (1977) vol. 7, p. 248; 16th Int. Cosmic-ray Conf. (1979) vol. 13, p. 82;

S.A. Azimov, E.Zh. Mullazhanov and T.S. Yuldashbayev, 16th Int. Cosmic-ray Conf. (1979) vol. 7, p. 262; Acta Univ. Lodz ser. II, no. 60 (1977) 275
Mt. Fuji experiment:
K. Kasahara, S. Torii and T. Yuda, 16th Int. Cosmic-ray Conf. (1979) vol. 13, pp. 70, 79;
M. Shibata, 16th Int. Cosmic-ray Conf. (1979) vol. 7, p. 176
Chacaltaya experiment:
H. Semba, T. Shibata and T. Tabuki, Suppl. Prog. Theor. Phys., to be published.

[7] G.B. Zhdanov, N.N. Roinishvilli, Yu.A. Smorodin and A. Tomaszevski, FIAN preprint no. 163 (1975)

[8] (a) C.M.G. Lattes, Y. Fujimoto and S. Hasegawa, Phys. Reports 65 (1980) 152
(b) R.W. Ellsworth, T.K. Gaisser and G.B. Yodh, Phys. Rev. D23 (1981) 764

[9] Pamir experiment:
L.T. Baradzei, Yu.A. Smorodin, FIAN preprint nos. 103, 104 (1974); Acta Univ. Lodz ser. II, no. 60 (1977) 51;
G.B. Zhdanov, FIAN preprint no. 140 (1980)
Chacaltaya experiment:
H. Semba, Suppl. Prog. Theor. Phys., to be published

[10] T. Shibata, Phys. Rev. D22 (1980) 100

[11] S.A. Slavatinsky, Proc. 7th European Symp. on Cosmic rays, Leningrad (1980), to be published; Brazil-Japan Emulsion Chamber Collaboration, AIP Conference Proc. no. 49 (1979) 145

[12] S.A. Azimov, Sh. Abduzhamilov, G.M. Chudakov et al., JETP (Sov. Phys.) 45 (1963) 407

[13] Brazil-Japan Emulsion Chamber Collaboration, 13th Int. Cosmic-ray Conf. (1973) vol. 5, p. 326

[14] B.S. Acharya, M.V.S. Rao, K. Sivaprasad, S. Rao, 16th Int. Cosmic-ray Conf. (1979) vol. 6, p. 289; R.W. Ellsworth, J. Goodman, G.B. Yodh, T.K. Gaisser and T. Stanev, Phys. Rev. D23 (1981) 771

[15] S.C. Bariburina, Z.M. Guseva, V.C. Denisova et al., Pamir Collaboration, Acta Univ. Lodz 1 (1980) 94

[16] Mt. Fuji Emulsion Chamber Group, 15th Int. Cosmic-ray Conf. (1977) vol. 7, p. 184; AIP Conf. Proc. no. 49 (1979) 334